 GRACE, Remote Sensing and Ground-based Methods in Multi-Scale Hydrology (Proceedings of Symposium J-H01 held during IUGG2011 in Melbourne, Australia, July 2011) (IAHS Publ. 343, 2011).

Monitoring surface and groundwater variations using multisatellite observations and hydrological modelling

FRÉDÉRIC FRAPPART[1], FRÉDÉRIQUE SEYLER[2], FABRICE PAPA[1], JEAN-MICHEL MARTINEZ[1], THUY LE TOAN[1], JOECILA SANTOS DA SILVA[3], CATHERINE PRIGENT[4] & WILLIAM B. ROSSOW[5]

1 *Université de Toulouse, Observatoire Midi-Pyrénées, 14 Avenue Edouard Belin, 31400 Toulouse, France*
frederic.frappart@get.obs-mip.fr

2 *IRD, US ESPACE, Montpellier, France*

3 *Universidade do Estado da Amazonas, Manaus, Brazil*

4 *CNRS, Observatoire de Paris, LERMA, Paris, France*

5 *NOAA, New York, USA*

Abstract We present a methodology combining information from complementary remote sensing datasets and hydrological modelling for the monitoring of surface and groundwater variations in two large drainage basins, the Negro and the Mekong rivers. Spatiotemporal variations of surface waters can be determined combining observations from satellite imagery (i.e. JERS-1, SPOT VGT, multisatellite products) and radar altimetry (i.e. Topex/Poseidon, ERS-1&2 RA, ENVISAT RA-2). The orbital characteristics and the type of sensors present advantages and drawbacks depending on the nature of the study region, and account for the spatial and temporal resolutions, and the accuracy of the surface water storage estimates. Water stored in aquifers is isolated from the total water storage measured by GRACE by removing the contributions of both the surface reservoir derived from satellite imagery and radar altimetry, and the root zone reservoir simulated by hydrological models.

Key words remote sensing; hydrological modelling; surface waters; groundwater

INTRODUCTION

Among the various reservoirs in which fresh water on land is stored (e.g. ice caps, glaciers, snowpack, soil moisture surface and groundwater), surface waters (rivers, lakes, reservoirs, wetlands and inundated areas) play a crucial role in the global biogeochemical and hydrological cycles (de Marsily *et al.*, 2005). Although wetlands and flood plains cover only 6% of the Earth's surface, they have a substantial impact on flood flow alteration, sediment stabilization, water quality, groundwater recharge and discharge (Maltby, 1991; Bullock & Acreman, 2003). Moreover, flood plain inundation is an important regulator of river hydrology owing to storage effects along channel reaches. Reliable and timely information about the extent, spatial distribution, and temporal variation of wetlands and floods, as well as the amount of water stored, is crucial to better understand their relationship with river discharges, and also their influence on regional hydrology and climate.

Remote sensing techniques have been very useful for studying the climate and hydrology of large river basins. Good capabilities for monitoring inundation extent using passive microwave measurements (Hamilton *et al.*, 2002), multispectral images (Osezmi & Bauer, 2002), SAR images (Hess *et al.*, 2003; Martinez & le Toan, 2007) or combining multisatellite information (Prigent *et al.*, 2007; Papa *et al.*, 2010), water levels and discharges using radar altimetry (Birkett, 1998; Frappart *et al.*, 2006a; Santos da Silva *et al.*, 2010), have already been demonstrated. The Gravity Recovery And Climate Experiment (GRACE) mission, launched in 2002, detects tiny changes in the Earth's gravity field, which can be related to the spatio-temporal variations of the terrestrial water storage (*TWS*) at 10-day or monthly time-scales (Tapley *et al.*, 2004). Variations in the groundwater storage can be separated from the *TWS* measured by GRACE using external information on the other hydrological reservoirs such as *in situ* observations (Yeh *et al.*, 2006), model outputs (Rodell *et al.*, 2009), or both (Leblanc *et al.*, 2009). No similar studies have been yet undertaken for large river basins characterized by extensive wetlands or flood plains.

In this paper, we propose a methodology to estimate water storage changes in large river basins by combining imagery-derived inundation extents, altimetry-derived water levels and

gravimetry from space products, and also soil water outputs from hydrological models. We present the analysis of surface water and groundwater storage variations in the Negro River and Mekong basins.

METHODOLOGY

Monthly water level maps

Monthly maps of water level over the flood plains of a large river basin can be determined by combining the observations from a satellite inundation data set, radar altimetry derived water levels, and *in situ* hydrographic stations for the water levels over rivers and flood plains (see Fig. 1 for the location of altimetry-based and *in situ* stations in the Negro and Mekong basins). The water levels are linearly interpolated over the flooded zones determined using satellite imagery. The elevation of each pixel of the water level maps is given with reference to its minimum computed over the observation period. This minimum elevation represents either the bathymetry or very low water stage of the flood plain. More details about the methodology used here can be found in Frappart *et al.* (2005, 2006b, 2008).

Groundwater storage estimates

The time variations of the *TWS* expressed as anomalies are the sum of the contributions of the different reservoirs present in a drainage basin:

$$\Delta TWS = \Delta SW + \Delta RZ + \Delta GW \quad (1)$$

where *SW* represents the total surface water storage including lakes, reservoirs, in-channel and flood plains water; *RZ* is the water contained in the root zone of the soil (representing a depth of 1 or 2 m), and *GW* is the total groundwater storage in the aquifers. These terms are generally expressed in volume (km^3) or mm of equivalent water height.

The *GW* anomaly is obtained in equation (1) by calculating the difference between the *TWS* anomaly from GRACE and the *SW* level anomaly maps previously derived from remote sensing and the *RZ* anomaly derived from hydrological models outputs. The *TWS* and *RZ* monthly anomalies are the average of the Level-2 GRACE products, and the outputs from LaD and WGHM, respectively. All the datasets were spatially resampled to 1 degree, and the monthly anomalies of each dataset were computed, removing its average over the 2003–2004 time period.

Water volume variations

For a given month *t*, the regional water volume of *TWS*, *SW*, *RZ* or *GW* storage $\delta V(t)$ in a basin with surface area *S*, is simply computed from the water heights δh_j, with $j = 1, 2, \ldots$ (expressed in mm of equivalent water height) inside *S*, and the elementary surface $R_e^2 \sin\theta_j \delta\lambda\delta\theta$ (and the percentage of inundation P_j for *SW* from the multisatellite inundation dataset):

$$\delta V(t) = R_e^2 \sum_{j \in S} P_j \delta h_j(\theta_j, \lambda_j, t) \sin\theta j \delta\lambda\delta\theta \quad (2)$$

where λ_j and θ_j are co-latitude and longitude, $\delta\lambda$ and $\delta\theta$ are the grid steps in longitude and latitude (generally $\delta\lambda = \delta\theta$), and R_e the mean radius of the Earth (6378 km). The surface and total water volume variations are expressed in km^3.

RESULTS AND DISCUSSION

Water levels time series

The altimetry stations where water level time series can be constructed (see Frappart *et al.*, 2005, 2006a; Santos da Silva *et al.*, 2010 for the methodology) are unevenly distributed across the Negro

and Mekong basins (Fig. 1). Due to their orbital characteristics, Topex/Poseidon (T/P) has a better temporal resolution but a larger intertrack spacing than ENVISAT RA-2 (10 against 35 days and 315 against 80 km near the equator).

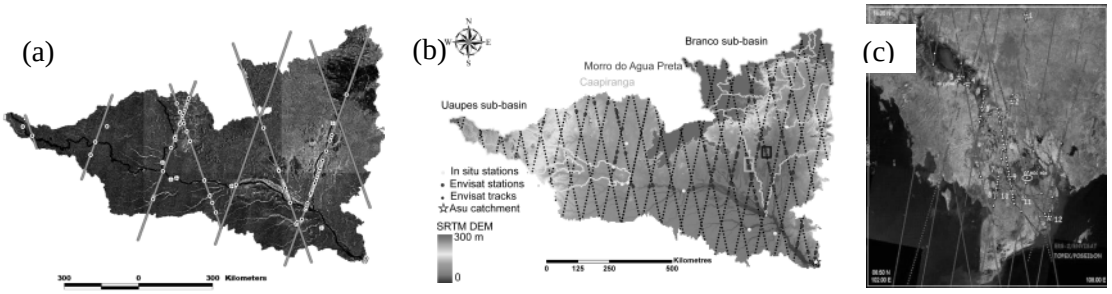

Fig. 1 Map of altimetry tracks and altimetric stations in the Negro and Mekong basins, (a) for T/P in the Negro basin, (b) for ENVISAT RA-2 in the Negro basin, (c) for T/P and ENVISAT RA-2 in the Mekong basin.

In the Negro basin, 86 T/P and 140 Envisat RA-2 altimetric stations corresponding to the intersection between the satellite tracks and rivers or flood plains were defined (Fig. 1(a) and (b)). In the Mekong basin, 80 Envisat RA-2 altimetric stations were defined (Fig. 1(c)). Envisat RA-2 orbit offers a better spatial sampling of the drainage basins than T/P at the expense of a lower temporal sampling. In the tropics, even for large drainage basins such as the Mekong (Fig. 1(c)), T/P is unable to provide a sufficient coverage of the river and its major tributaries.

Altimetric stations permit monitoring of the time variations of water levels both on rivers and flood plains to be monitored with accuracy greater than 50 cm for T/P and 30 cm for RA-2. The better accuracy of RA-2 derived water levels compared with T/P comes from two major reasons. First, T/P was dedicated to the measurement of ocean surface topography whereas RA-2 is devoted to the monitoring of all types of the Earth's surfaces. As a consequence, T/P often lost radar echoes over land, especially for low water stages. Second, T/P echoes were only tracked onboard to estimate the altimeter range (i.e. the distance between the satellite and the surface) whereas ENVISAT Geophysical Data Records (GDR) contains four different estimates of the altimeter range, each of them corresponding to a specific retracking process. Frappart *et al.* (2006a) showed that the Ice-1 retracking scheme was the more suitable for land hydrology.

Inundation extent and surface water volume

Different types of satellite images can be used to delineate floods. In the different cases presented in this paper, SAR, multispectral images and a multisatellite product were employed to characterize the spatio-temporal variations of the flood (Fig. 2). The SAR images, such as the JERS-1 double mosaic used in the Negro basin (Frappart *et al.*, 2005), presents the major advantages of (i) a high spatial resolution (~100 m for JERS-1 double mosaic), (ii) to be used whatever the weather conditions, and (iii) to be able to detect, in C or L band for instance, the presence of water under the forest canopy. Nevertheless, they do not offer a sufficient temporal repetitivity to be used to monitor flood extent at subseasonal time-scales. In the Negro basin, they allowed the flood type (permanent, non-permanent, non-flooded) of each pixel to be characterized and, combined with T/P altimetry-derived water levels, to map the water levels over the rivers and tributaries (Fig. 2(a)), and to estimate the maximum surface water volume stored at the sub-basin scale during the 1995–1996 hydrological cycle. This last result, compared with the measured volume of water that flowed during the same period, provides important information on the residence time of the surface in each sub-basin. The ALOS PALSAR L-band sensor, launched in 2006 by JAXA, now provides images at 100 m of resolution, with a 46-day repeat cycle, at a regional scale, which are very helpful to monitor inundation during the annual hydrological cycle.

The multisatellite inundation dataset (Prigent *et al.*, 2007; Papa *et al.*, 2010), which provides the monthly average inundated areas fraction in a pixel of approximately 25 × 25 km^2, was also used to characterize the flood in the Negro basin over the period 1993–2004 of common availability of T/P and ENVISAT RA-2 radar altimetry datasets, and of the multisatellite inundation product (Frappart *et al.*, 2008, 2011). It allowed the interannual variations of inundated surfaces and surface water volume to be quantified. Inundation and surface water level maps (Fig. 2(b)) exhibit realistic patterns: seasonal and interannual variabilities are consistent with precipitation and river discharges, especially during ENSO years.

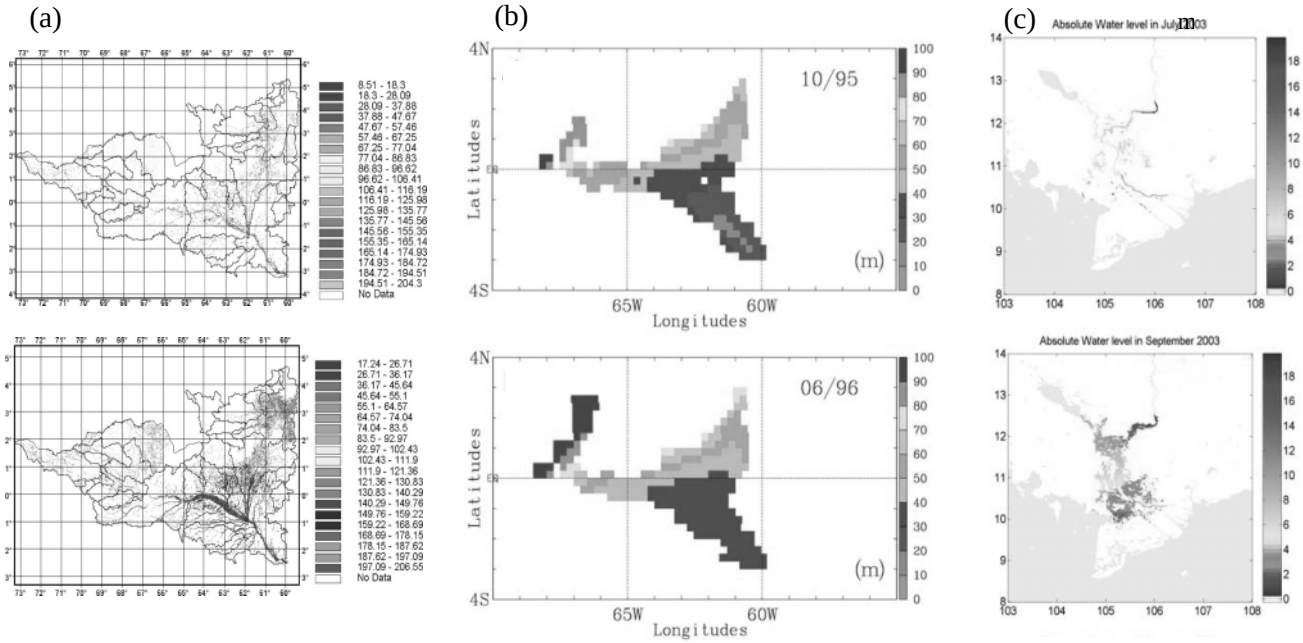

Fig. 2 Map of surface water levels: (a) using JERS-1 and T/P in the Negro basin – low water 1995 (top) and high water 1996 (bottom), (b) using the multisattelite inundation and T/P in the Negro basin – October 1995 (top) and June 1996 (bottom), (c) using SPOT-VGT and ENVISAT RA-2 in the Mekong basin – July 2003 (top) and September 2003 (bottom).

Comparisons have been made with the results obtained by Frappart *et al.* (2005) for the 1995–1996 hydrological cycle. Due to the coarse resolution of the multisatellite product, the flood in the upstream parts of the Negro River and its major tributaries was not detected (Fig. 2(a) and (b)). Considering the same study area, annual surface volume variation from the multisatellite product and T/P is 30% lower than the maximum storage variations estimated using JERS-1 and T/P. The difference in the maximum surface water storage variations between the two methods derives primarily from biases in the flooded area estimates of both multisatellite and SAR products (Frappart *et al.*, 2008).

Medium resolution (1 km) *NDVI* 10-day synthetic images (S10) from SPOT-VGT were used to delineate flood extent in the Mekong basin. To reduce residual cloud contamination, the maximum extent of the flood during the month maps were computed from the union of the three 10-day flood maps (see examples in Fig. 2(c)). An extensive analysis of the basin surface properties show that a pixel can be considered inundated if its *NDVI* value is lower than 0.2. Combined with ENVISAT RA-2 altimetry derived water levels, they allowed us to monitor at monthly time-scales the floods between July and December over the period 1996–2004 (Frappart *et al.*, 2006b). The major drawbacks of multispectral images are the impossibility to detect water under dense vegetation cover and the sensitivity to clouds.

Time variations of the *GW* anomaly

Time variations (and deviation at each time step) of the water storage anomalies in the *TWS*, *SW*, *RZ* and *GW* reservoirs for 2003 and 2004 were estimated in the Negro basin (Fig. 3(a)). The deviations correspond to the extreme values of GRACE-derived *TWS* from Level-2 CSR, GFZ and JPL solutions and associated errors, of *RZ* from WGHM and model outputs, and of *SW*, taking into account errors in inundated surfaces and heights. The *TWS* signal is dominated during the high waters (May to July) by the *SW* variations (Frappart *et al.*, 2011). The *RZ* varies in phase with both *TWS* and *SW*, and the amplitude of its variations represents a third of the amplitude of *TWS* variations, which is similar to what was obtained by Kim *et al.* (2009) for the whole Amazon basin. The resulting *GW* variations exhibit a more complex profile with two peaks. Its time variations follow the bimodal distribution of the precipitation resulting from the geographical location of the basin in both hemispheres (Fig. 1(b)). A large variability, reaching several months, is observed in the timing of the extremes across the basin: *GW* storage is maximum (minimum) in July–August (December–March) in the western part (Uaupes and west of the Negro), in June–July (February to April) in the centre of the basin and the downstream of the Branco, in August–September in the upper part of the Branco, and in May–June (October–December) for the downstream part of the Negro basin. These results are consistent with *in situ* measurements from sites located in the downstream part of the Negro basin (Do Nascimento *et al.*, 2008; Tomasella *et al.*, 2008) and are closely related to the timing of *GW* recharge and the soil thickness. In Manaus, the time-lag between the maxima of rainfall and *GW* is 3 months, which is similar to what is observed with *in situ* measurements.

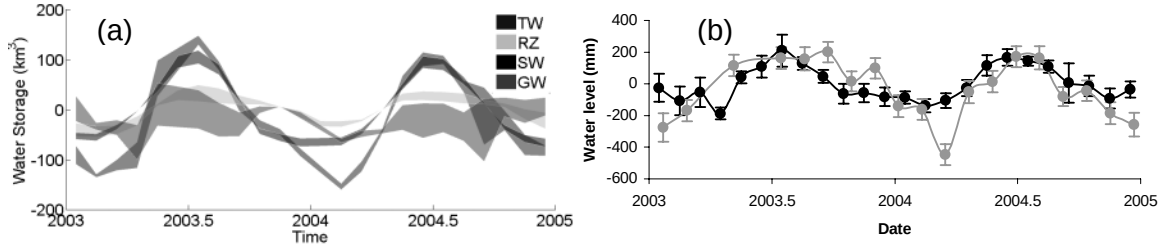

Fig. 3 (a) Time variations of the water storage contained in the different hydrological reservoirs: *TWS*, *RZ*, *SW*, *GW*. (b) Time variations of the surface water levels (grey) and the groundwater (black) in the swamps of Caapiranga.

The groundwater table permanently reached the surface in several parts of the Negro basin. Two of these regions, the Caapiranga and Morro da água preta swamps (Fig. 1(b)), are flooded and can be monitored using radar altimetry. In these cases, we expect *GW* to have similar time variations as water levels. A time series of *SW* and corresponding *GW* anomalies over 2003–2004 are presented in Fig. 3(b) for Caapiranga. Except for February 2004, where the *SW* derived from radar altimetry present an abnormally low level (larger errors on altimetry-derived stages during the low water season, due to the presence of dry land or vegetation in the satellite field of view, have been also observed in different studies (see for instance Frappart *et al.*, (2006a) or Santos da Silva *et al.*, (2010)), both time series agree well (R = 0.76 for Caapiranga and 0.73 for Água do Morro Preta) and exhibit similar temporal patterns and amplitudes.

CONCLUSION

The combination of dense altimetry-based water levels with satellite imagery provides an interesting new methodology for remotely measuring surface water volumes over extensive flood plains in large river basins. This combination provides valuable information on the dynamics of

the inundation of river flood plains in large river basins. These results are also of great interest for the preparation of the future wide swath altimetry mission SWOT (Surface Water and Ocean Topography) that will measure 2-D water levels at a spatial resolution of 1 km over a 120 km swath. The complementarity between remote sensing derived hydrological products (altimetry, imagery and gravimetry from space) allowed us to estimate the time variations of the total soil storage. Adding information from hydrological modelling, we were able to estimate realistic time variations of the anomaly of water contained in the aquifers of a large river basin characterized with extensive flood plains.

REFERENCES

Birkett, C. M. (1998) Contribution of the TOPEX NASA radar altimeter to the global monitoring of large rivers and wetlands *Water Resour. Res.* **34**(5), 1223–1239.

Bullock, A. & Acreman, M. (2003) The role of wetlands in the hydrological cycle. *Hydrol. Earth Syst. Sci.* **7**, 358–389.

Do Nascimento, N. R., Fritsch, E., Bueno, G. T., Bardy, M., Grimaldi, C. & Melfi, A. J. (2008) Podzolization as a deferraltization process: dynamics and chemistry of ground and surface waters in an Acrisol – Podzol sequence of the upper Amazon basin. *European J. Soil Sci.* **59**, 911–924.

Frappart, F., Martinez, J. M., Seyler, F., León, J. G. & Cazenave, A. (2005) Flood plain water storage in the Negro River basin estimated from microwave remote sensing of inundation area and water levels. *Remote Sens.Environ.* **99**(4), 387–399.

Frappart, F., Calmant, S., Cauhopé, M., Seyler, F. & Cazenave, A. (2006a) Preliminary results of ENVISAT RA-2 derived water levels validation over the Amazon basin. *Remote Sens. Environ.* **100**(2), 252–264.

Frappart, F., Do Minh, K., L'Hermitte, J., Cazenave, A., Ramillien, G., Le Toan, T. & Mognard-Campbell, N. (2006b) Water volume change in the lower Mekong basin from satellite altimetry and imagery data. *Geophys. J. Int.* **167**(2), 570–584.

Frappart, F., Papa, F., Famiglietti, J. S., Prigent, C., Rossow, W. B. & Seyler, F. (2008) Interannual variations of river water storage from a multiple satellite approach: a case study for the Rio Negro River basin. *J. Geophys. Res.* **113**(D21), D21104.

Frappart, F., Papa, F., Güntner, A., Werth, S., Santos da Silva, J., Tomasella, J., Seyler, F., Prigent, C., Rossow, W. B., Calmant, S. & Bonnet, M. P. (2011). Total water storage decomposition and estimates of groundwater variations in the Negro River Basin *Remote Sens. Env.* **115**(6), 1588–1594.

Hamilton, S. K., Sippel, S. J. & Melack, J. M. (2002) Comparison of inundation patterns among major South American flood plains. *J. Geophys. Res.* **107**(D20), 10.129–10.143.

Hess, L. L., Melack, J. M., Novo, E. M. L. M., Barbosa, C. C. F. & Gastil, M. (2003) Dual-season mapping of wetland inundation and vegetation for the central Amazon basin *Remote Sens. Env.* **87**(4), 404–428.

Kim, H., Yeh, P. J.-F., Oki, T. & Kanae, S. (2009) Role of rivers in the seasonal variations of terrestrial water storage over global basins. *Geophys. Res. Lett.* **36**, L17402.

Leblanc, M. J., Tregoning, P., Ramillien, G., Tweed, S. O. & Fakes, A. (2009) Basin-scale, integrated observations of the early 21st century multiyear drought in southeast Australia. *Water Resour. Res.* **45**, W04408.

Maltby, E. (1991) Wetland management goals: wise use and conservation. *Landscape Urban Plann.* **20**, 9–18.

de Marsily, G. (2005) Eaux continentals. *C. R. Geosci.* **337**, 1–2.

Martinez, J-M. & Le Toan, T. (2007) Mapping of flood dynamics and spatial distribution of vegetation in the Amazon flood plain using multitemporal SAR data. *Remote Sens. Environ.* **108**(3), 209–223.

Ozesmi, S. L. & Bauer, M. E. (2002) Satellite remote sensing of wetlands. *Wetlands Ecol. Manage.* **10**, 381–402.

Papa, F., Prigent, C., Aires, F., Jimenez, C., Rossow, W. B. & Matthews, E. (2010) Interannual variability of surface water extent at global scale. *J. Geophys. Res.* **115**, D12111.

Prigent, C., Papa, F., Aires, F., Rossow, W. B. & Matthews, E. (2007) Global inundation dynamics inferred from multiple satellite observations. 1993–2000. *J. Geophys. Res.* **112**, D12107.

Roddel, M., Velicogna, I. & Famiglietti, J. (2009) Satellite-based estimates of groundwater depletion in India. *Nature* **460**, 999–1003.

Santos da Silva, J., Calmant, S., Seyler, F., Rottuno Filho, O. C., Cochonneau, G. & Mansur, W. J. (2010) Water levels in the Amazon basin derived from the ERS 2 and ENVISAT radar altimetry missions. *Remote Sens. Environ.* **114**(10), 2160–2181.

Tapley, B. D., Bettadpur, S., Watkins, M. M. & Reigber, C. (2004) The Gravity Recovery and Climate Experiment; mission overview and early results. *Geophys. Res. Lett.* **31**(9), L09607.

Tomasella, J., Hodnett, M. G., Cuartas, L. A., Nobre, A. D., Waterloo, M. J. & Oliveira, S. M. (2008) The water balance of an Amazonian micro-catchment: the effect of interannual variability of rainfall on hydrological behaviour. *Hydrol. Processes* **22**, 2133–2147.

Yeh, P. J.-F., Swenson, S. C., Famiglietti, J. S. & Rodell, M. (2006) Remote sensing of groundwater storage changes in Illinois using the Gravity Recovery and Climate Experiment (GRACE). *Water Resour. Res.* **42**, W12203.